Poly(acrylic acid)-*block*-poly(L-valine): Evaluation of β-Sheet Formation and Its Stability Using Circular Dichroism Technique

A. Sinaga,[†] T. A. Hatton,[†,§] and K. C. Tam*[,†,‡,||]

Singapore-MIT Alliance National University of Singapore E4-B-07/8, 4 Engineering Drive 3, Singapore 117576, School of Mechanical and Aerospace Engineering, Nanyang Technological University, Singapore 639798, and Department of Chemical Engineering, Massachusetts Institute of Technology, Cambridge, Massachusetts 02139

Received May 6, 2007; Revised Manuscript Received June 26, 2007

Secondary structure formation in four novel hybrid poly(acrylic acid)-*b*-poly(L-valine) (PAA-b-PLVAL) block copolymers, that is, PAA_{40}-$PLVAL_{100}$, PAA_{80}-$PLVAL_{100}$, PAA_{80}-$PLVAL_{80}$, and PAA_{80}-$PLVAL_{60}$, was investigated by circular dichroism. The formation of stable and well-defined β-sheet structure in the PLVAL hydrophobic domains was observed for all the copolymers. At pH 5, PAA_{80}-$PLVAL_{60}$ with the lowest PLVAL/PAA molar ratio possessed the lowest β-sheet content of 12%, and it increased to 62% for PAA_{40}-$PLVAL_{100}$ system. The β-sheet formation in the block copolymers was controlled by both random PAA-PLVAL hydrogen bonds at low pH and electrostatic repulsive forces on the PAA segment at high pH; hence, the β-sheet structure was most stable at intermediate pH. The length of PAA segments was critical in the β-sheet solubilization and in providing sufficient shielding of the hydrophobic core from denaturing agents such as urea.

Introduction

The preparation of hybrid systems containing conventional synthetic polymeric segments and poly(L-amino acids) allows the combination of desired properties, such as solubility, melt processability, rubber elasticity of the synthetic block, and structural formation, mutual recognition, high mechanical performance, or biodegradability from the peptide block.[1] Current studies on hybrid block copolymers between a conventional synthetic polymer segment (e.g., PEO,[2,3] polybutadiene,[4,5] poly(lactide),[6] etc.) and linear sequences of amino acid revealed interesting properties since the amino acid segment introduces additional factors through specific noncovalent interactions (secondary structure effects) and their directional polarity and chirality.[7,8] Such additional factors may result in the formation of hierarchical superstructures with adjustable properties and functionalities. Furthermore, conformational transition between different secondary structures (α-helix, β sheet, and random coil) can be utilized to produce a change in material properties in response to environmental stimuli, such as pH and temperature.[9−11]

β-sheet formation has been identified as an important component that contributes to the comprehensive mechanical properties of natural silks, for example, spider and silkworm silks, that are superior to artificial materials. The structure of silk is made up of a cross-linked, amorphous polymer network composed of glycine-rich blocks reinforced by a well-orientated crystalline filler composed of alanine-rich blocks.[12,13] Novel biomaterials that incorporate the precise control of the architecture exhibited by silk proteins are usually achieved by the replacement of the glycine-rich block by synthetic oligomers such as PEG[14,15] or isoprene.[16] These synthetic polymers, however, can dissolve only in polar organic solvents such as hexafluoro-2-propanol, dichloroacetic acid, or $CHCl_3$/2-chloroethanol,[16] hence their applications are limited to film-casting applications. Furthermore, the intractable nature of these β-sheet-forming amino acid sequences has severely limited the study and use of such hybrid block copolymers for applications in aqueous solutions, for example, as drug/gene carriers.

In this article, a novel block copolymer system comprising a β-sheet-forming hydrophobic poly(L-valine) and a charged poly(acrylic acid), that is, PAA-*block*-PLVAL, was examined. Such a hybrid block copolymer system between charged conventional polymers and hydrophobic poly(L-amino acids) has not been explored previously. In particular, the conjugation of the poly(acrylic acid) segment was demonstrated to enhance the solubility of β-sheet-forming poly(L-valine), signifying the potential of using charged polymers to increase the processability of β-sheet forming materials and hence allowing the wider use of such motifs for advanced materials. Four polymers of different compositions, namely, PAA_{40}-$PLVAL_{100}$, PAA_{80}-$PLVAL_{100}$, PAA_{80}-$PLVAL_{80}$, and PAA_{80}-$PLVAL_{60}$, were synthesized, and the formation of ordered secondary structure was elucidated at different pH conditions. Secondary β-sheet structures were observed for all four copolymers, and their stability and β-sheet content are dependent on both the PLVAL/PAA molar ratio and pH. At high pH, lower β-sheet content was observed for all polymers because of the presence of electrostatic charge repulsions from deprotonated COOH groups, which hinder the close packing of the polymeric chains. In addition, β-sheet formation was also disrupted at low pH through the formation of random hydrogen bonds with PAA segments. The length of the PAA segment, however, was demonstrated to be critical in providing a steric shield for the β-sheet structure in the hydrophobic domain of the polymers and hence minimizing their disruption by external chemical agents such as urea.

* Corresponding author. Fax: 519-746-4979. E-mail: mkctam@uwaterloo.ca.
† Singapore-MIT Alliance National University of Singapore.
‡ Nanyang Technological University.
§ Massachusetts Institute of Technology.
|| Current address: Department of Chemical Engineering, University of Waterloo, Waterloo, Ontario, Canada N2L 3G1.

10.1021/bm700491q CCC: $37.00
Published on Web 08/21/2007

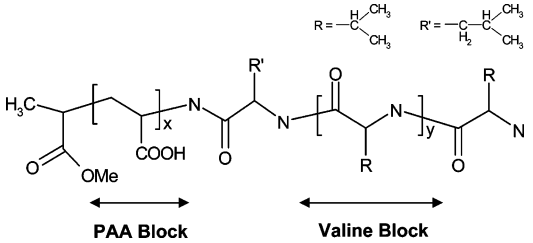

Figure 1. Chemical Structure of PAA-*block*-PLVAL.

Experimental Procedures

Materials. Four PAA-*block*-PLVAL copolymers were synthesized through the combined approach of ATRP, Click chemistry, and nickel-catalyzed polymerization of *N*-carboxyanhydrides of L-valine. The chemical structure of the block copolymers is shown in Figure 1.

All chemical reagents were purchased from Sigma-Aldrich and were used without further purifications unless otherwise specified. The *t*BA monomer was passed through a column of basic alumina to remove any acidic contaminants, dried under calcium hydride, and subsequently distilled under reduced pressure. THF and hexane were dried by heating with sodium strips and calcium hydride, respectively, under reflux condition for 3 days. DMF was dried using molecular sieves and then degassed by three freeze−thaw cycles to remove oxygen.

A detailed description of the synthetic approach for the hybrid block copolymers was reported previously.[17] The overall synthetic scheme of the block copolymers is shown in Scheme 1, followed by a brief description of the experimental procedures.

Synthesis of Poly(*tert*-butyl acrylate) (b). A reaction (Schlenk) flask was sealed with a rubber septum, degassed and dried, and back-filled with argon. Deoxygenated methyl-2-bromo propionate, CuBr, and $CuBr_2$ were then added to the flask in a 2:1:0.05 mol ratio. The required amount of *t*BA monomer and deoxygenated acetone (30 vol % of *t*BA) was added to the reaction flask via an argon-washed syringe. This was followed by three freeze−thaw cycles to remove any traces of oxygen from the reaction system. Deoxygenated PMDETA (1:1 mol ratio with CuBr) was subsequently added, and the solution was stirred to form the Cu complex. The reaction solution at this stage changed from colorless and cloudy to dark green. The flask was then transferred to a thermostated oil bath at 60 °C and left overnight to obtain the polymer with the designed molecular weight. The crude polymer was subsequently purified by passing through a neutral alumina column, stirred with ion-exchange resin for 1−2 h, and precipitation in a 50:50 water/methanol mixture (yield = 80 wt %). ^{1}H NMR ($CDCl_3$): 1.1 ppm (t, initiator C*H*$_3$ group), 1.5 ppm (broad, -CH_2-CH(COO-C(C*H*$_3$)$_3$)-, *t*BA), 1.9 ppm (m, -C*H*$_2$-CH(COO-C(CH$_3$)$_3$)-, *t*BA), 2.3 ppm (m, -CH_2-C*H*(COO-C(CH$_3$)$_3$)-, *t*BA), 3.5−3.6 ppm (-OC*H*$_3$, intiator), 3.8 ppm (end group proton). IR (KBr pellet): 2981, 2937, 1734, 1483, 1458, 1394, 1367, 1261, 1157, 846, 754 cm^{-1}.

Synthesis of Azide ω-Functional Poly(*tert*-butyl acrylate) (c). Thirty mol excess of sodium azide was dissolved in DMF to make an approximately 0.03 M solution. Poly(*tert*-butyl acrylate) was then added to the solution, and the azidation reaction was allowed to occur for 8 h at room temperature. The reaction was concentrated by distillation under reduced pressure and subsequently precipitated in a 50:50 water/methanol mixture (yield = 98%). ^{1}H NMR ($CDCl_3$): 1.1 ppm (t, initiator C*H*$_3$ group), 1.5 ppm (broad, -CH_2-CH(COO-C(C*H*$_3$)$_3$)-, *t*BA), 1.9 ppm (m, -C*H*$_2$-CH(COO-C(CH$_3$)$_3$)-, *t*BA), 2.3 ppm (m, -CH_2-C*H*(COO-C(CH$_3$)$_3$)-, *t*BA), 3.5−3.6 ppm (−OC*H*$_3$, intiator; end-group proton). IR (KBr pellet): 2100 cm^{-1} (-N_3 vibration).

Synthesis of Amino ω-Functional Poly(*tert*-butyl acrylate) (d) by Click Chemistry. Compound **c** (0.8 mmol, 4 g), CuBr (3× mol equiv), and bipyridine (6× mol equiv) were added into a reaction flask that was capped with a septum and purged with argon. Degassed THF was added from an argon-washed syringe to produce a homogeneous dark

Scheme 1. Synthesis Scheme of PAA-*block*-PLVAL Hybrid Polymers

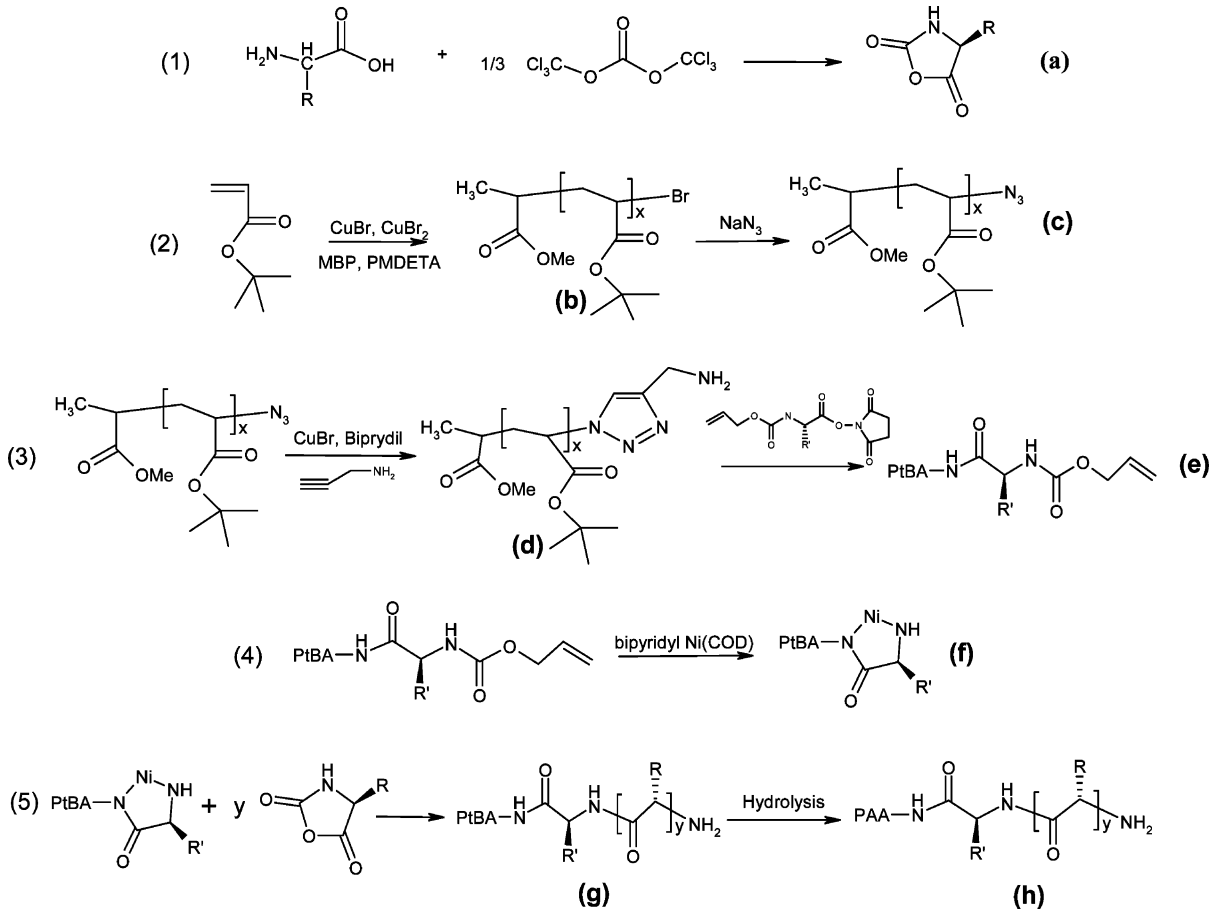

brown solution. The reaction mixture was subsequently freeze−thawed for 3 cycles to completely remove dissolved oxygen. Degassed propargyl amine (3× mol equiv) was then added, and the reaction mixture was stirred overnight at room temperature. The product was purified by passing the reaction mixture through an alumina column and precipitated into water at pH 5 (yield = 97%). ^{1}H NMR ($CDCl_3$): 1.1 ppm (t, initiator C*H*$_3$ group), 1.5 ppm (broad, -CH$_2$-CH(COO-C(C*H*$_3$)$_3$)-, *t*BA), 1.9 ppm (m, -C*H*$_2$-CH(COO-C(CH$_3$)$_3$)-, *t*BA), 2.3 ppm (m, -CH$_2$-C*H*(COO-C(CH$_3$)$_3$)-, *t*BA), 3.7 ppm (−OC*H*$_3$, initiator), 6.9 ppm (triazole proton). IR (KBr pellet): 3450, 2981, 2937, 2368, 1734, 1483, 1458, 1394, 1367, 1261, 1157, 846, 754 cm^{-1}.

Synthesis of Poly(*tert*-butyl acrylate) Macroinitiator (f). Compound **d** (0.2 mmol, 1.1 g) was added to a solution of **e** (1 mol equiv) in 5 mL of dry THF. The reaction mixture was stirred overnight at room temperature. The *N*-hydroxysuccinimide side product was removed by filtration, and the reaction mixture was concentrated under vacuum. Fifteen milliliters of ethyl acetate was added to dilute the crude mixture, and extraction was done with saturated bicarbonate, dilute HCl, and NaCl solutions. The solution was then dried with $MgSO_4$ and the product recovered by solvent removal under vacuum (yield = 92%). ^{1}H NMR ($CDCl_3$): 0.9 ppm (-CH$_2$-CH-(C*H*$_3$)$_2$), 1.1 ppm (t, initiator C*H*$_3$ group), 1.5−1.8 ppm (m, -C*H*$_2$-C*H*-(CH$_3$)$_2$), 1.5 ppm (broad, -CH$_2$-CH(COO-C(C*H*$_3$)$_3$)-, *t*BA), 1.9 ppm (m, -C*H*$_2$-CH(COO-C(CH$_3$)$_3$)-, *t*BA), 2.3 ppm (m, -CH$_2$-C*H*(COO-C(CH$_3$)$_3$)-, *t*BA), 4.4 ppm (t, -NH-C*H*(C$_4$H$_9$)-COO-), 4.6 ppm (s, CH$_2$=CH-C*H*$_2$-), 5.3 ppm (d, C*H*$_2$=CH-CH$_2$-), 5.9 ppm (m, CH$_2$=C*H*-CH$_2$-), 6.9 ppm (triazole proton).

Synthesis of Hybrid Poly(*tert*-butyl acrylate)-*block*-poly(L-valine) (g). In a glove box, 0.05 g of Ni(COD)$_2$ metal catalyst was weighed and dissolved in 0.6 mL of DMF. Separately, a solution of equimolar solution of bipyridine in DMF was prepared and subsequently mixed with the Ni solution. The mixture quickly turned into a dark purple solution, which was left to stir for an additional 3 h. One gram of macroinitiator **f** was dissolved in 1.2 mL of DMF and transferred to the purple solution to form a solution of the initiating metal complex **g** with a final concentration of 40 mM. This solution was heated at 80 °C for 24 h.

For the polymerization, a 0.1 g/mL solution of the required amount of valine NCA in DMF was prepared. The metal complex solution was then transferred by an argon-washed syringe into the solution to start the copolymerization. The reaction was allowed to proceed for 48 h at room temperature after which it was concentrated and precipitated into cold methanol containing 1 mM HCl. The precipitation procedure was repeated three times to ensure the complete removal of unreacted macroinitiator (yield = 78%). ^{1}H NMR (d_7-DMF): 0.9−1 ppm (dd, -CH-(C*H*$_3$)$_2$, valine), 1.5 ppm (broad, -CH$_2$-CH(COO-C(C*H*$_3$)$_3$)-, *t*BA), 1.9 ppm (m, -C*H*$_2$-CH(COO-C(CH$_3$)$_3$)-, *t*BA), 2.3 ppm (m, -CH$_2$-C*H*(COO-C(CH$_3$)$_3$)-, *t*BA). IR (KBr pellet): 1654 cm^{-1} (amide I band).

Synthesis of Hybrid Poly(acrylic acid)-*block*-poly(L-valine) (g). Hydrolysis of the *tert*-butyl acrylate side group was carried out under room temperature. A 10 wt % solution of the copolymer in dicholoromethane was prepared in a round-bottom flask. Following this, trifluoroacetic acid (10 mol excess of *t*BA groups) was added to the solution, and the reaction was allowed to proceed overnight. The solution was concentrated by rotary evaporation and the product purified by precipitation into hexane (overall yield = 55% mol of original ATRP initiator). ^{1}H NMR (d_6-DMSO): 0.9−1 ppm (dd, -CH-(C*H*$_3$)$_2$, valine), 1.9 ppm (m, -C*H*$_2$-CH(COOH)-, PAA), 2.3 ppm (m, -CH$_2$-C*H*(COOH)-, PAA). IR (KBr pellet): 1654 cm^{-1} (amide I band). ^{1}H NMR IR (KBr pellet): 3000−3700 cm^{-1} (broad COOH band), 1720 cm^{-1} (-C=O), 1654 cm^{-1} (amide I band).

Table 1 summarizes the composition, polydispersity index (PDI), and percent hydrolysis of the polymers. The percent hydrolysis refers to the percent conversion of the deprotected reaction that generates the COOH groups from the initial *tert*-butyl acrylate protecting groups. As can be observed from Table 1, the percent hydrolysis of all copolymers was greater than 94%, and hence, we would expect minimal contribution from the hydrophobic *tert*-butyl acrylate group toward the self-assembly of the block copolymers.

Table 1. Molecular Composition and Polydispersity Index (PDI) of PAA-*block*-PLVAL

polymer	x	Y	MW[a]	PDI[b]	% hydrolysis[c]
1	80	100	15600	1.18	96.2%
2	80	80	13700	1.21	95.3%
3	80	60	11700	1.17	94.1%
4	40	100	12800	1.24	97.1%

[a] MW obtained from NMR in d_7-DMF. [b] PDI was determined from GPC of the corresponding poly(*t*BA)-PLVAL prior to hydrolysis; column temperature = 60 °C; eluent = 1% LiBr in DMF; elution rate = 1 mL/min. [c] % hydrolsis was determined from the acid−base potentiometric titration.

Sample Preparation. Prior to preparing the test solutions, the block copolymer obtained from the synthesis was additionally purified by dialysis in deionized water. Typically, the polymers were dissolved in deionized water at a concentration of 0.5 wt % and transferred to a regenerated cellulose dialysis membrane (Snake Skin Pleated Dialysis Tubing) with a molecular weight cutoff of 3500 Da. Dialysis was carried out for one week with deionized water that was replaced every 12 h. The polymers were then freeze-dried to yield a white powder that was readily redispersed in deionized water. Polymer stock solutions of 1 wt % and pH 10 were then prepared and stored in a freezer, and sample solutions at the required concentrations were subsequently prepared by diluting the stock solution with a pre-filtered deionized water (with a 0.2 μm nylon membrane filter). The solutions were then adjusted to a final NaCl salt concentration of 0.2 M, using a 2 M NaCl stock solution, and to the required pH of between 5 and 10 using dilute 0.1 M NaOH or HCl solution. All samples were equilibrated overnight prior to physical characterizations to ensure that the self-assembly process has reached an equilibrium.

Instrumentation. *Circular Dichroism (CD)*. The formation of ordered secondary structures in the copolymer aggregates was examined using an Olis rapid scanning monochromator at room temperature. The path length of the quartz cell is 0.1 mm and a PLVAL concentration of 0.3 g/L was used. This concentration roughly corresponds to about 0.4−0.6 g/L of the block copolymers depending on their PLVAL/PAA composition. Blank solutions with each of the corresponding pH and urea and salt concentration were used as the background, and the CD spectra were deconvoluted using a Contin II approach to obtain the relative composition of the different secondary structures. All spectra were scanned from a wavelength of 190−250 nm at a 0.5 nm stepsize.

Potentiometric Titration. An ABU93 Triburet Titration System equipped with Radiometer pHG201 pH glass and Radiometer REF201 reference electrodes was used to conduct potentiometric and conductometric titrations. All titrations were performed under constant stirring at 25 °C, in a 100 mL titration vessel. The polymer solutions were prepared at a concentration of 0.1 wt % and a pH of 10. One molar standard HCl and NaOH solutions were then used for the forward acid titration and backward base titration, respectively. A lag time of 1 min was allowed between two consecutive dosages to ensure that the neutralization reaction had reached equilibrium. The degree of ionization of the polymers, α, was then calculated as $[COO^-]/[COOH]_{total}$.

Results and Discussion

Composition-Dependent Formation of β-Sheet in PAA-*block*-PLVAL Polymers. To identify the type and subsequently quantify the degree of formation of ordered secondary structures within the hydrophobic domains of the four block copolymers, circular dichroism (CD) spectroscopy was used. CD is experimentally the most convenient method to determine the secondary structure of proteins and polypeptides; therefore, CD was extensively applied to the structural characterization of these

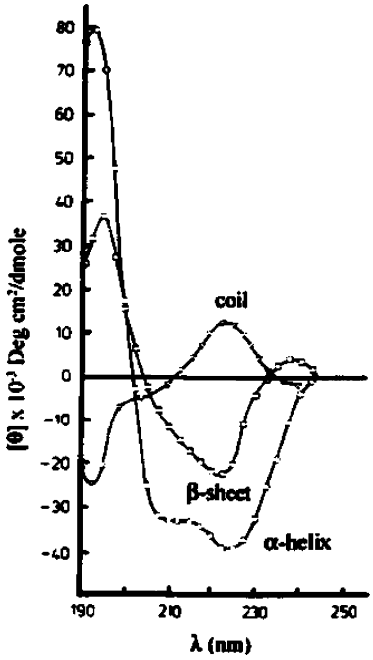

Figure 2. Characteristic CD bands of secondary structures in proteins and polypeptides.[18]

materials. Generally, CD measurements rely on the difference in the absorbance between right and left circularly polarized light by an aqueous solution of optically active molecules. An examination of CD spectra of these molecules, then, allows the determination of the type of ordered structures through the presence of characteristic CD bands. Figure 2 shows characteristic CD bands for the three secondary structures commonly found for poly(peptides) and proteins.[18]

The PLVAL segment of the block copolymers is hydrophobic and has been known to form insoluble β-sheet secondary structure. However, the PAA segments do not possess any chiral centers and hence do not exhibit any specific CD signals. Therefore, all of the CD spectra of the polymers were collected at the same PLVAL weight concentration of 0.3 g/L, whereas the total polymer concentration ranged between 0.4 and 0.6 g/L, depending on the PLVAL/PAA composition. This is to avoid any possible effect that slight variations of total PLVAL concentration may have on the extent of formation of the ordered structure. Furthermore, comparison of CD spectra should be carried out at the same degree of neutralization, α, of the PAA segment to avoid variations due to different charge densities between the different polymer compositions. The degree of neutralization, α, of the block copolymers can be defined as the fraction of COOH groups that exists in their deprotonated form, that is, as COO^- groups, and was measured by potentiometric titration of the polymers. Figure 3 shows the dependence of pH on the α of the solutions.

A comparison of the CD spectra of the polymers at the same degree of neutralization, α of 0.3, can be observed in Figure 4. The PAA_{80}-$PLVAL_{80}$, PAA_{80}-$PLVAL_{100}$, and PAA_{40}-$PLVAL_{100}$ systems formed core−shell micellar structures with aggregation number increasing in that particular order, whereas the PAA_{80}-$PLVAL_{60}$ system existed only as random aggregates or unimeric state.

It can be seen from the figure that PAA_{40}-$PLVAL_{100}$ exhibited characteristic β-sheet CD bands, namely, a positive band at about 195 nm and a negative band at about 217 nm.[18] Compared to Figure 2, however, the negative CD band of the PAA_{40}-$PLVAL_{100}$ sample exhibited a slight broadening to a wavelength

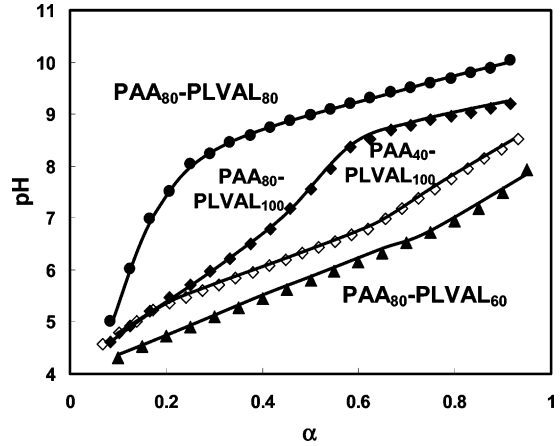

Figure 3. Dependence of the degree of neutralization (α) of PAA-*block*-PLVAL polymers with pH.

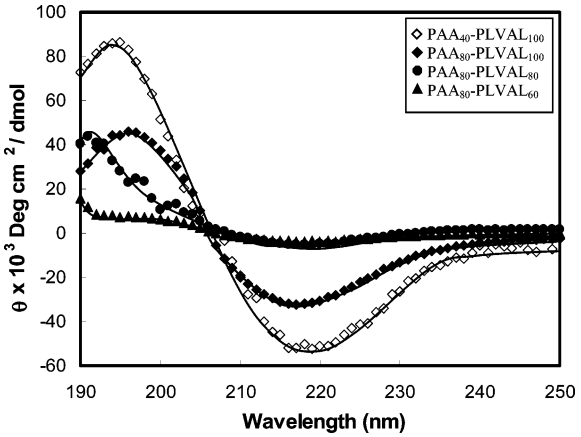

Figure 4. Analysis of the formation of secondary structure of PAA_{40}-$PLVAL_{100}$, PAA_{80}-$PLVAL_{100}$, PAA_{80}-$PLVAL_{80}$, and PAA_{80}-$PLVAL_{60}$ at $\alpha = 0.3$ through circular dichroism.

of about 221 nm, which is an indication of the presence of other secondary structures. On reducing the PLVAL/PAA molar ratio to 3:4 (for PAA_{80}-$PLVAL_{60}$), the intensity of both the positive and negative bands were decreased and a shift of the positive band toward lower wavelength was observed. This behavior showed that there was a lowering of the stability and the extent of β-sheet formation at lower PLVAL/PAA molar ratios, which was also reflected in the decrease of aggregation number of the corresponding micelles. Also, the PAA_{80}-$PLVAL_{60}$ sample at 0.3 g/L PLVAL and $\alpha = 0.3$ precipitated after 2 days. However, the self-assembled structure of the remaining three polymers were stable, and no significant change in the CD spectra was observed after 3 days. The observed precipitation of the PAA_{80}-$PLVAL_{60}$ system may be related to its inability to form closed aggregate structures (e.g., micellar structures) because of its lower hydrophobic character compared to that of the other three polymers. Since the PLVAL segment is nonetheless capable of forming intermolecular hydrogen bonds, we believed that the polymer chains associated to form random large aggregates that subsequently precipitated out of solution. The reduction in the concentration and/or increase in the pH of PAA_{80}-$PLVAL_{60}$ samples resulted in CD signals that were very close to the signal of a blank solution (background) showing that the polymer was possibly in an unaggregated state. Hence, the behavior of PAA_{80}-$PLVAL_{60}$ will not be discussed further because it did not form a well-defined self-assembled structure.

pH-Dependent Formation of β-Sheet in PAA-*block*-PLVAL Polymers. Quantitative information regarding the

formation of ordered structures in the polymer could be obtained through the deconvolution of the CD spectra into separate contributions from the possible individual secondary structures, namely, β-sheet (regular and distorted), α-helix (regular and distorted), β-turns, and random coils. A CONTIN program was used for this purpose, where the experimental data were fitted to a linear construct of CD data of standard proteins (43 soluble proteins and 13 membrane proteins) whose precise secondary structures are already known through X-ray crystallography.[19] Briefly, the CD spectra of the samples can be estimated as a linear sum of N_t different CD spectra of reference proteins as follows:

$$y(\lambda) = \sum_{j=1}^{N_t} \gamma_j R_j(\lambda) \quad (1)$$

where $y(\lambda)$ is the mean ellipticity signal, at a wavelength of λ; γ_j is the fractional contribution of the CD spectrum of reference protein j at a wavelength of λ; and $R_j(\lambda)$ is the mean residual ellipticity of the CD spectrum of reference protein j at a wavelength of λ.

The fraction of residues of the samples existing in a particular conformational class i, that is, the six possible secondary structures, can then be estimated from F_{ji}, the fraction of residues of reference protein j in that particular class as obtained from their X-ray structure.

$$f_i = \sum_{j=1}^{N_t} \gamma_j F_{ji} \quad (2)$$

Generally, we have no a priori knowledge of γ_j values, that is, the relative contribution of each of the reference $R_j(\lambda)$ values. Therefore, it is initially necessary to assign an equal fractional contribution of each of the reference spectra ($\gamma_{j,0} = 1/N_t$) unless there is a justified preference to some γ_j values, for example, when the protein sample is of a known family. The deviation of this initial theoretical construct of CD spectra from the experimental data was then analyzed in terms of a modified least-square equation.

$$\sum_{k=1}^{N_y} [y(\lambda_k) - y_{obsd}(\lambda_k)]^2 + \alpha \sum_{j=1}^{N_t} \left(\gamma_j - \frac{1}{N_t}\right)^2 \quad (3)$$

where $y_{obsd}(\lambda_k)$ is the observed mean ellipticity at a particular data point (i.e., at $\lambda = \lambda_k$), and N_y is the total data points in the experimental CD spectra. The second term in the equation can be considered as a correction term to the least-square approach, as usually a large set of reference spectra, N_t, was used for the deconvolution process. The α variable is a regularization parameter that ensures the stability and reliability of the estimated $\gamma_{j\ values}$ toward experimental errors while still having sufficient degrees of freedom to maintain model flexibility and prevent γ_j values that are too biased toward $1/N_t$. The selection of the optimum α in the analysis is generally associated with the set of reference proteins used in the fitting process. Nostrand et al. had previously discussed in great detail the procedures for choosing the optimum α for a particular set of reference proteins.[20] The fractions of the secondary structures in the samples were then obtained from the minimization of eq 3 with the constraints.

$$f_i \geq 0 \text{ and } \sum_{i=1}^{6} f_i = 1 \quad (4)$$

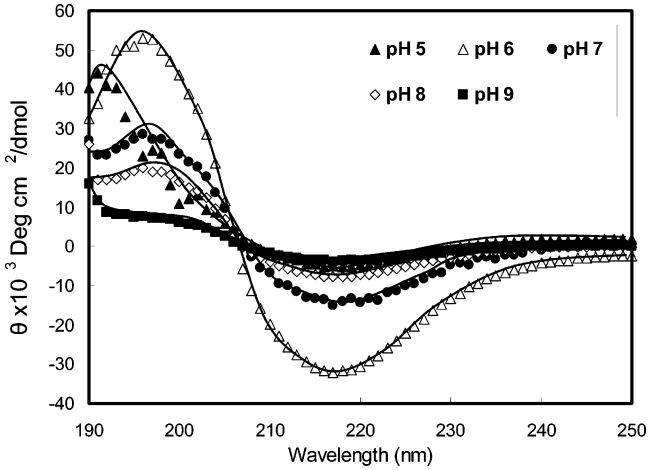

Figure 5. Effects of pH on the extent of β-sheet formation in the PAA_{80}-$PLVAL_{80}$ system.

Table 2. Quantification of the Formation of the Secondary Structure of PAA_{40}-$PLVAL_{100}$ (0.3 g/L PLVAL) at pH Range = 5−9

secondary structure	$\alpha = 0.29$ (pH 5)	$\alpha = 0.54$ (pH 6)	$\alpha = 0.79$ (pH 7)	$\alpha = 0.9$ (pH 8)	$\alpha = 0.94$ (pH 9)
regular helix (%)	0.2	2.0	0.9	0.4	0.6
distorted helix (%)	1.9	0.7	1.4	1.5	1.0
regular β sheet (%)	51.4	44.8	34.5	28.7	23.5
distorted β sheet (%)	11.1	11.9	13.9	10.1	11.2
β turns (%)	16.5	16.8	16.6	17.7	16.3
unordered (%)	19.3	23.8	32.3	41.5	49.2
total helix (%)	2.1	2.7	2.3	1.9	1.6
total β-sheet (%)	62.5	56.7	48.4	38.8	35.7

The CD spectra as a function of degree of neutralization, α, were plotted in Figure 5 for PAA_{80}-$PLVAL_{80}$ to illustrate the trend observed for the three polymeric systems. The results for the deconvolution of the CD spectra for PAA_{40}-$PLVAL_{100}$, PAA_{80}-$PLVAL_{100}$, and PAA_{80}-$PLVAL_{80}$ at different α and the corresponding actual solution pH values are summarized in Tables 2 through 4. The deconvolution of the PAA_{80}-$PLVAL_{60}$ sample ($\alpha = 0.3$) showed a β-sheet content of about 12% with the remaining in a random coil state. It should be mentioned here that the aggregation number of the block copolymer micelles was constant with pH, while the changes in the β-sheet content with pH reflected the internal rearrangements of the polymer chains in the micelle needed to compensate for the increase in polymer charge density. The specific roles of the β-sheet structure in the size and regularity and the unique properties it afforded to the core−shell micelles are currently being investigated and will be the subject of subsequent publications.

The general effect of increasing pH toward the formation of ordered secondary structures can be seen from changes of CD spectra within pH 6−9 (Figure 5) and more clearly from the data in Tables 2−4. It can be observed from Tables 2−4 that the β-sheet structure is the dominant secondary structure at all pH values for the three polymers. When the pH of the solution was increased, the COOH groups of the PAA segment became increasingly deprotonated and charged, which consequently resulted in an increase in the intermolecular electrostatic repulsion between the polymeric chains. This intermolecular repulsion, in turn, prevented the close packing and parallel alignment of the polymer molecules in a β-sheet structure and therefore resulted in a reduction in the total β-sheet content of all three polymers at high pH. However, we noted that the helix contents of the three polymers were unchanged with pH, which indicated that these helices possibly existed as a localized coiling

Table 3. Quantification of the Formation of the Secondary Structure of PAA_{80}-$PLVAL_{100}$ (0.3 g/L PLVAL), pH Range = 5−10

secondary structure	$\alpha = 0.1$ (pH 5)	$\alpha = 0.17$ (pH 6)	$\alpha = 0.26$ (pH 7)	$\alpha = 0.5$ (pH 8)	$\alpha = 0.75$ (pH 9)	$\alpha = 1$ (pH 10)
regular helix (%)	1.2	1.2	2.0	0.8	0.1	0.6
distorted helix (%)	2.3	2.5	2.6	2.3	3.2	2.5
regular β sheet (%)	35.8	38.2	32.5	29.4	24.8	18.4
distorted β sheet (%)	19.2	17.9	18.1	14.8	18.1	16.7
β turns (%)	20.7	19.7	21.2	20.7	21.0	11.7
unordered (%)	21.2	20.8	23.6	32.0	32.8	50.1
total helix (%)	3.5	3.7	4.6	3.1	3.3	3.1
ltotal β-sheet (%)	55.0	56.1	50.6	44.2	42.9	35.1

Table 4. Quantification of the Formation of the Secondary Structure of PAA_{80}-$PLVAL_{80}$ (0.3 g/L PLVAL, pH Range = 5−10)

secondary structure	$\alpha = 0.12$ (pH 5)	$\alpha = 0.3$ (pH 6)	$\alpha = 0.44$ (pH 7)	$\alpha = 0.54$ (pH 8)	$\alpha = 0.75$ (pH 9)	$\alpha = 1$ (pH 10)
regular helix (%)	1.2	1.4	1.1	1.5	0.9	0.1
distorted helix (%)	2.5	2.6	2.3	2.5	2.1	2.3
regular β sheet (%)	37.2	42.5	33.0	30.2	27.9	17.2
distorted β sheet (%)	13.5	8.3	10.2	10.1	10.7	13.1
β turns (%)	19.7	19.5	20.8	19.9	19.2	21.3
unordered (%)	25.8	25.6	32.6	36.4	39.5	47.1
total helix (%)	3.7	4.0	3.4	4.0	3.0	2.4
total β-sheet (%)	50.7	50.8	43.2	40.3	38.6	30.3

of only a few amino acid units in the PLVAL segment rather than as an extended structure.

Comparison of the β-sheet formation at the same degree of neutralization, α, showed that there was no significant difference in the β-sheet content in the PAA_{40}-$PLVAL_{100}$ and PAA_{80}-$PLVAL_{100}$ systems at higher α regions, that is, at $\alpha > 0.75$. This was particularly interesting since it was expected that the higher electrostatic repulsion in PAA_{80}-$PLVAL_{100}$ due to the longer PAA segment and consequently the higher amounts of charges per polymeric chain would result in a lower β-sheet formation at all pH ranges. Therefore, this observation suggested that there is a similar core β-sheet bonded region in both polymer systems that remained unperturbed by charge repulsion. This core region is presumably formed by the chain ends furthest from the hydrophobic−hydrophilic interface. Furthermore, this core region was also thought to be essential for the self-assembly of the polymer systems since the PAA_{80}-$PLVAL_{60}$ system that exhibited only 12% β sheet content could not form well-defined aggregates as discussed earlier.

A second interesting observation for the PAA_{40}-$PLVAL_{100}$ and PAA_{80}-$PLVAL_{100}$ systems is the increasing difference in β-sheet content between the two systems at low α regions, from 6% at $\alpha = 0.75$ to 17% difference at $\alpha = 0.29$, though their PLVAL segments were of equal length. This difference could not be explained through charge repulsion only since there should be a lower charge density at low α. Furthermore, it can also be observed that the β-sheet content of PAA_{40}-$PLVAL_{100}$ was more affected by the pH change than PAA_{80}-$PLVAL_{100}$, which is in contradiction to what would be expected if the observed variation was due to charge repulsion only since the latter system possessed a longer PAA segment. Therefore, there must be an additional destabilizing factor that dominated at low pH, and this might be attributed to the ability of COOH groups on PAA segments to undergo hydrogen bonding with the amide groups on the PLVAL segment, thereby replacing the required PLVAL−PLVAL hydrogen bonds and hence disrupting the β-sheet arrangement. This conclusion was further supported by the CD spectra of PAA_{80}-$PLVAL_{80}$ in Figure 5, which exhibited a reverse pH trend with the intensity of both the positive and negative bands increasing as the pH was increased from 5 to 6 (indicative of a higher β-sheet content) in contrast to the general destabilizing effect of pH discussed earlier.

The subtle interplay between the destabilizing effects of random PAA−PLVAL hydrogen bonding and charged repulsion can also be demonstrated from a closer observation of the PAA_{80}-$PLVAL_y$ systems (Tables 3 and 4), where the β-sheet structure was further classified into a regular or distorted structure. It is obvious for the two polymers that there is a conversion/stabilization of some of the distorted β-sheet structure into a more regular structure as the pH was increased from 5 to 6 (with α changing from around 0.1 to 0.3). It can be hypothesized here that the introduction of a small amount of charge into the system induced the release of COOH groups that were initially buried in the hydrophobic region because of the random hydrogen bonding with PLVAL units, which subsequently facilitated a closer and tighter molecular packing while also releasing more amide groups to form the ordered β-sheet structure. Alternatively, it is also possible that the pH increase in this region caused the deprotonation of COOH groups from some of the amide/COOH hydrogen-bond pairs, resulting in the formation of a more ordered structure.

Figure 6 shows a schematic of the cross-section of the local hydrophobic region of PAA_{80}-$PLVAL_y$ block copolymer systems ($y = 80$ or 100), where the proposed changes in the β-sheet formation and stability due to electrostatic charges on the PAA segment are illustrated. Destabilization of the β-sheet structure occurred at both low pH because of the formation of random hydrogen bonds with COOH groups (Figure 6A) and at high pH because of charge repulsions (Figure 6C) as discussed previously. The illustrated bending of PAA segments to form hydrogen bonds with the PLVAL segments in the hydrophobic region in Figure 6A requires the PAA segment to be of sufficient length and flexibility, which explains the absence of such a destabilizing effect in the PAA_{40}-$PLVAL_{100}$ systems, where the PAA length is only half that of the PAA_{80}-$PLVAL_y$ systems.

In light of the CD results, the observed trends in the potentiometric titration of the different polymers can be explained in terms of the existence of the PAA−PLVAL

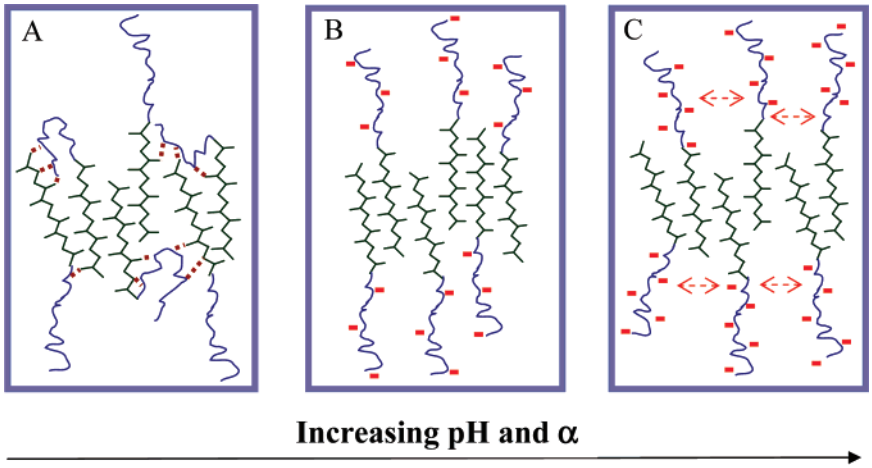

Figure 6. Changes of local β-sheet formation of PAA_{80}-$PLVAL_y$ ($y = 80$ or 100). (A) Existence of COOH/amide hydrogen bonds (brown dotted lines) due to the buried PAA segments that reduce the packing efficiency and disrupt β-sheet formation. (B) Introduction of sufficient charge releases PAA segment, allowing the polymer molecules to be more closely realigned and more PLVAL hydrogen bonds to form, resulting in a more regular β-sheet structure. (C) Further increase in charge enhances repulsion between PAA segments, which disrupts the β-sheet structure at the interface between the hydrophobic domain and the surrounding aqueous environment.

hydrogen bonds. For the PAA_{40}-$PLVAL_{100}$ system, there was only minimal effect from these hydrogen bonds since the length of the PAA segment was too short to be intercalated into the hydrophobic PLVAL core. Furthermore, because of the asymmetry in the PAA and PLVAL lengths and differences in their aqueous solubilities, there is a very high tendency and preference for the PLVAL and PAA blocks to self-aggregate (or phase separate) into domains that were predominantly composed of either the PLVAL in the hydrophobic micellar core or the PAA segment in the micellar shell. However, as the PAA/PLVAL ratio increased to 1, that is, as the composition was changed from PAA_{40}-$PLVAL_{100}$ to PAA_{80}-$PLVAL_{100}$, and then to PAA_{80}-$PLVAL_{80}$, the formation of random PAA/PLVAL hydrogen bonds was enhanced, which subsequently reduced the aggregation tendency between like segments, resulting in less defined core−shell interface regions and significant mixing and interaction between the PAA and PLVAL segments. Furthermore, this reduced the accessibility of COOH groups from the aqueous NaOH base since these COOH groups were more shielded within the compact hydrophobic core of the aggregates during the neutralization process. Hence, we observed an increase in the barrier for the overall proton dissociation process as reflected by the trend in the polymer titrations where there were higher pH requirements for the PAA_{80}-$PLVAL_{80}$ system in order to reach the same α as that of the PAA_{80}-$PLVAL_{100}$ system, which also in turn required higher pH compared to that of the PAA_{40}-$PLVAL_{100}$ system (Figure 3).

The observed lowest pH requirement for the PAA_{80}-$PLVAL_{60}$ system can also be explained by the reduced aggregation tendency as we further increased the PAA/PLVAL molar ratio. Because of its lack of hydrophobicity and low β-sheet content, the system did not form well-defined polymeric micelles, and thus, the titration results reflected the individual unimeric state, which behaved in the same manner, as if they were linear strands of polyelectrolytes with no observed effect of the PLVAL segment.

Stability of the β-Sheet in PAA-*block*-PLVAL Polymers in the Presence of Urea. Urea, $CO(NH_2)_2$, is known to be a strong denaturing agent for the disruption of hydrogen bonds and the unfolding of protein materials. In order to investigate the accessibility of the β-sheet network formed by the three block copolymer systems, urea was added in 0.1 M increments until the polymer aggregates were completely dissociated, as

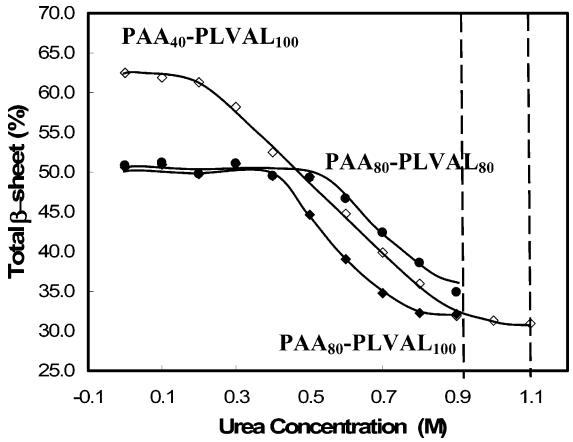

Figure 7. Dependence of total β-sheet content of the block copolymers with total urea concentration (0.3 g/L PLVAL segment, $\alpha = 0.3$). The maximum urea concentrations before the complete dissociation of polymer aggregates are indicated by the dotted lines.

indicated by the absence of any CD signals above the solution background absorbance. Also, it should be stressed that precipitation of the polymers, which would also result in the absence of the CD signal, was not observed. The experiments were carried out at $\alpha = 0.3$, where the β-sheet formation was at its optimum. Figure 7 shows the changes in the total β-sheet content from the deconvolution of CD spectra as a function of total urea concentration for the PAA_{40}-$PLVAL_{100}$, PAA_{80}-$PLVAL_{80}$, and PAA_{80}-$PLVAL_{80}$ systems.

From Figure 7, it can be observed that prior to the complete dissociation of polymer aggregates at a urea content of about 0.9 M, all three polymers exhibited similar total β-sheet contents of around 32%. Therefore, it seemed that the aggregation of polymeric chains is dependent on the formation of critical total β-sheet content, below which the micellar aggregate was not thermodynamically stable. In addition, Figure 7 shows that the hydrophobicity of the polymer played a role in stabilizing the micellar aggregate because the most hydrophobic system of PAA_{40}-$PLVAL_{100}$ remained stable up to a higher urea concentration of 1.1 M.

The effects from the addition of urea on β-sheet formation was observed to be more substantial for the PAA_{40}-$PLVAL_{100}$ system because the β-sheet content of this system began to decrease at 0.3 M of urea, whereas the β-sheet formation in the

PAA_{80}-$PLVAL_y$ systems was not being disrupted. Since the length of the PAA segment in PAA_{40}-$PLVAL_{100}$ was only half that of the PAA_{80}-$PLVAL_y$ ($y = 80$ or 100), it can be thought that the β-sheet domains in the former system were more accessible compared to that of the latter. This hypothesis was further supported by the comparison of PAA_{80}-$PLVAL_y$ systems. The shorter PLVAL segment of the PAA_{80}-$PLVAL_{80}$ system was observed to result in a slightly lower accessibility of its β-sheet domain compared to that of the PAA_{80}-$PLVAL_{100}$ system since the size of the β-sheet domain in the former system will be smaller and better shielded by its PAA segment. Therefore, an optimum PAA/PLVAL length ratio would exist where there is minimum disruption of β-sheet formation, either from random hydrogen bonds or charge repulsions, by the PAA segment while still maintaining proper shielding of the β-sheet domains from its surrounding environment.

Conclusions

The formation of ordered β-sheet secondary structures in the hydrophobic domains of four different hybrid PAA-*block*-PLVAL of varying compositions, namely, PAA_{40}-$PLVAL_{100}$, PAA_{80}-$PLVAL_{100}$, PAA_{80}-$PLVAL_{80}$, and PAA_{80}-$PLVAL_{60}$, was described. A common critical core β-sheet content of approximately 30% was identified for the hybrid polymer systems below which the formation of well-defined and stable polymer aggregates was not possible. The PAA_{80}-$PLVAL_{60}$ system, which exhibited 12% β-sheet content, existed only as unstable random aggregates at pH < 5 and in an unaggregated state at higher pH.

The stability of the ordered β-sheet structure in the block copolymer system was found to be dependent on three related factors, namely, the degree of charge repulsion, the extent of the interference of hydrogen bonds with the PAA segment, and the polymer composition. In general, the formation of β-sheet structure was improved and stabilized at an intermediate pH, where there was minimal interference from random PAA−PLVAL hydrogen bonds and minimal repulsive effects from surface charges that prevent close packing of the polymeric chains. The formation of the β-sheet was also stabilized as the PLVAL/PAA molar ratio was increased since both charge effects and the interference of hydrogen bonds were reduced. However, it was found that the length of the PAA segment was also important, particularly as a steric shield for the hydrophobic β-sheet core, which minimized the accessibility and prevented the disruption of the core by external denaturing chemical agents, such as urea.

Acknowledgment. We acknowledge Dr. P. Ravi for his help in the developmental stage of the block copolymer synthesis and Dr. Wilmouth and Wu Binhui from the School of Biological Sciences, NTU, for their assistance with the circular dichroism experiments. We also thank the Singapore-MIT Alliance for financial support in the form of a graduate scholarship.

Supporting Information Available. Details on the characterization of PAA-*block*-PLVAL polymers, namely, FTIR and NMR . This information is available free of charge via the Internet at http://pubs.acs.org.

References and Notes

(1) Vandermeulen, G. W. M.; Klok, H. A. *Macromol. Biosci.* **2004**, *4*, 383.
(2) Toyotama, A.; Kugimiya S.-I.; Yamanaka, J.; Yonese, M. *Chem. Pharm. Bull.* **2001**, *49*, 169.
(3) Kwon, G. S.; Naito, M.; Yokoyama, M.; Okano, T.; Sakurai, Y.; Kataoka, K. *Langmuir* **1993**, *9*, 945.
(4) Kukula, H.; Schlaad, H.; Antonietti, M.; Förster S. *J. Am. Chem. Soc.* **2002**, *124*, 1658.
(5) Chécot, F.; Brûlet, A.; Oberdisse, J.; Gnanou, Y.; Mondain-Monval, O.; Lecommandoux, S. *Langmuir* **2005**, *21*, 4308.
(6) Arimura, H.; Ohya, Y.; Ouchi, T. *Biomacromolecules* **2005**, *6*, 720.
(7) Cornelissen, J. J. L. M.; Rowan, A. E.; Nolte R. J. M.; Sommerdijk, N. A. J. M. *Chem. Rev.* **2001**, *101*, 4039.
(8) Lowik, D. W. P. M.; van Hest, J. C. M. *Chem. Soc. Rev.* **2004**, *33*, 234.
(9) Breedveld, V.; Nowak, A. P.; Sato, J.; Deming, T. J. *Macromolecules* **2004**, *37*, 3943.
(10) Holowka, E. P.; Pochan, D. J.; Deming, T. J. *J. Am. Chem. Soc.* **2005**, *127* (35), 12423.
(11) Rodriguez-Hernandez, J.; Lecommandoux, S. *J. Am. Chem. Soc.* **2005**, *127*, 2026.
(12) Lawrence, B. A.; Vierra, C. A.; Mooref, A. M. F. *Biomacromolecules* **2004**, *5*, 689.
(13) Jin, H. J.; Kaplan, D. L. *Nature (London*) **2003**, *424*, 1057−1061.
(14) Winningham, M. J.; Sogah, D. Y. *Macromolecules* **1997**, *30*, 862.
(15) Rathore, O.; Sogah, D. Y. *J. Am. Chem. Soc.* **2001**, *123*, 5231.
(16) Zhou, C.; Leng, B.; Yao, J.; Jie, Q.; Xin, C.; Ping, Z.; Knight D. P.; Shao, Z. *Biomacromolecules* **2006**, *7*, 2415.
(17) Sinaga, A.; Ravi, P.; Hatton, T. A.; Tam, K. C. *J. Polym. Sci., Part A: Polym. Chem.*, **2007**, *45*, 2646.
(18) Walton, A. *Polypeptides and Protein Structure*; Elsevier: New York, 1981.
(19) Provencher, S. W.; Gloeckner, J. *Biochemistry* **1981**, *20*, 33.
(20) Draper, N. R.; Van Nostrand, R. C. *Technometrics* **1979**, *21*, 451.

BM700491Q